A broadband polygonal cloak for acoustic wave designed with linear coordinate transformation

A broadband polygonal cloak for acoustic wave designed with linear coordinate transformation

Rongrong Zhu and Bin ZhengChu Ma, Jun Xu, and Nicholas FangHongsheng ChenMFH

Citation: The Journal of the Acoustical Society of America **140**, 95 (2016); doi: 10.1121/1.4954762
View online: http://dx.doi.org/10.1121/1.4954762
View Table of Contents: http://asa.scitation.org/toc/jas/140/1
Published by the Acoustical Society of America

A broadband polygonal cloak for acoustic wave designed with linear coordinate transformation

Rongrong Zhu and Bin Zheng[a)]
The Innovative Institute of Electromagnetic Information and Electronic Integration, Department of Electronic Engineering, Zhejiang University, Hangzhou, 310027, China

Chu Ma, Jun Xu, and Nicholas Fang
Department of Mechanical Engineering, Massachusetts Institute of Technology, 77 Massachusetts Avenue, Cambridge, Massachusetts 02139-4307, USA

Hongsheng Chen
The Innovative Institute of Electromagnetic Information and Electronic Integration, Department of Electronic Engineering, Zhejiang University, Hangzhou, 310027, China

(Received 1 December 2015; revised 28 April 2016; accepted 13 June 2016; published online 6 July 2016)

Previous acoustic cloaks designed with transformation acoustics always involve inhomogeneous material. In this paper, a design of acoustic polygonal cloak is proposed using linear polygonal transformation method. The designed acoustic polygonal cloak has homogeneous and anisotropic parameters, which is much easier to realize in practice. Furthermore, a possible acoustic metamaterial structure to realize the cloak is proposed. Simulation results on the real structure show that the metamaterial acoustic cloak is effective to reduce the scattering of the object.
 [http://dx.doi.org/10.1121/1.4954762]

[MFH] Pages: 95–101

I. INTRODUCTION

The concept of transformation optics[1,2] opens ways to control electromagnetic waves to achieve the invisibility cloak.[1–12] This coordinate-transformation-based method can also be extended to other physical systems, including acoustics. Thus, using the technique named transformation acoustics,[13–16] acoustic cloaking[17–28] can also be achieved. Significant progress has been made to realize the acoustic cloak practically. An underwater acoustic cloak for ultrasound waves was experimentally realized by a network of anisotropic acoustic transmission lines.[22] An acoustic ground cloak in air was also proposed using perforated plastic plates and works in two dimensions.[24] Furthermore, a three-dimensional ground cloak was designed and fabricated.[26] Most recently, an acoustic cloak was demonstrated which can work for acoustic, electromagnetic, and water waves simultaneously.[27]

The main difficulties encountered in implementing the cloaking devices may be due to the inhomogeneous and extremely anisotropic parameters after coordinate transformation. The concept of "carpet cloak" was proposed with quasi-conformal mapping method[4] to avoid the anisotropic parameters. However, the cloak still needs inhomogeneous construction and involves lateral shift of the reflected waves. Using the linear transformation method,[29] one can get homogeneous and anisotropic parameters for the cloaking devices. This method has been used in many carpet cloaks working for electromagnetic[7,8,30,31] and acoustic[23–26] waves. Polygonal[32] and polyhedral[33] transformation methods are also proposed for electromagnetic waves and then applied to acoustics. A two-dimensional rhombic acoustic cloak is reported with homogeneous constitutive parameters, but it only works for unidirectional incident waves.[34] Using a two-step linear transformation method, an omnidirectional diamond acoustic cloak has also been proposed,[35] however, the parameters of that are hard for practical realization.

In this paper, we propose a design of an omnidirectional acoustic polygonal cloak by applying linear transformation on a polygonal region. The designed cloak has simple parameters that can be realized with commercially available materials. Simulation results on the real structure shows that the cloak fabricated with the designed unit cells is effective at reducing the scattering from the object and works in a broad frequency band.

II. DESIGN METHOD

The linear transformation method was proposed[36] to design a hexagonal cloak for visible light. The cloak was divided into several regions with the parameter of each region to be anisotropic but homogeneous. In this paper, a similar transformation is applied to achieve a triangular cloak for acoustic waves. Figure 1 shows the transformation of the cloak from virtual space to physical space. In Fig. 1(a), a triangle region with a circumradius of r_2 is used in a virtual coordinate space, which is filled with isotropic material of density $\rho = \rho_0$ and bulk modulus $B = B_0$. In the center is a much smaller triangle with a circumradius of r_0 rotated at an angle of $\pi/3$ compared to the outer triangle. The space between the two triangles is

a)Electronic mail: zhengbin@zju.edu.cn

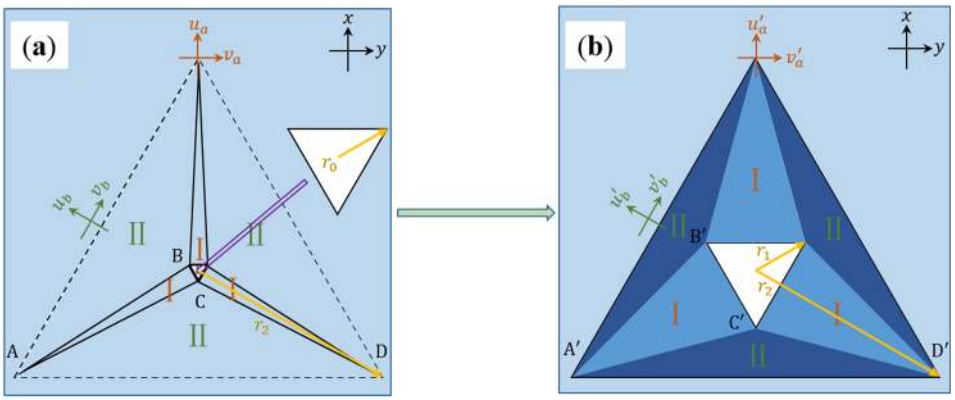

FIG. 1. (Color online) Illustration of linear transformation method. (a) Virtual space filled with isotropic materials with a small triangular object is divided into several segments. (b) Physical space constructed by the transformed segments with a big triangular object. The circumradius of the small object, big object and the outline of the cloak is r_0, r_1, and r_2, respectively.

divided by several triangular segments that can be grouped into two types due to the structure symmetry, marked as segment I and segment II. The two segments have their own local orthogonal coordinate axis, $(\bar{u}_a, \bar{v}_a, \bar{w}_a)$ and $(\bar{u}_b, \bar{v}_b, \bar{w}_b)$, respectively, where $\bar{w}$ is the direction perpendicular to the uv-plane.

A coordinate transformation is then applied in all segments along their own local axes to expand the center small triangle with a circumradius of r_0 to a bigger triangle with a circumradius of r_1, while the outer triangle with a circumradius of r_2 remains unchanged, as seen in Fig. 1(b). For example, for segment I, the triangle region ABC in virtual space is transformed to the triangle region A′B′C′ in physical space; while for segment II, the triangle region ACD in virtual space is transformed to the triangle region A′C′D′ in physical space. The other regions will be similar due to the symmetry. The transformation equations for each segment are

$$\begin{aligned} &\text{For segment I}: \ u'_a = u_a/\kappa_u,\ v'_a = \kappa_v v_a,\ w'_a = w_a, \\ &\text{For segment II}: \ u'_b = u_b/\kappa,\ v'_b = v_b,\ w'_b = w_b, \end{aligned} \tag{1}$$

where, κ_u, κ_v, and κ are ratios of compression or extension for the corresponding segments. For the triangle case, $\kappa_u = (r_2 - r_0/2)/(r_2 - r_1/2)$, $\kappa_v = r_1/r_0$ and $\kappa = (r_2/2 - r_0)/(r_2/2 - r_1)$, respectively.

The transformation shows that the hidden object, a triangle with circumradius of r_1, is mapped to a triangle with a much smaller circumradius of r_0, thus, it makes the object more difficult to be detected.

III. SIMULATION RESULTS

The parameters of the cloak can be obtained under the transformation shown in Eq. (1). If only the acoustic wave in the xy-plane is considered, we can get the following parameters for each segment:

$$\begin{aligned} &\text{For segment I}: \ \rho_u^{I'} = \rho_0\kappa_u\kappa_v, \rho_v^{I'} = \rho_0/\kappa_u\kappa_v, B^{I'} = B_0\kappa_v/\kappa_u, \\ &\text{For segment II}: \ \rho_u^{II'} = \rho_0\kappa, \rho_v^{II'} = \rho_0/\kappa, B^{II'} = B_0/\kappa. \end{aligned} \tag{2}$$

From Eq. (2), we find that the density of each segment is homogeneous, which can simplify the practical realization of the acoustic cloak. Numerical simulation is performed using finite element methods with COMSOL MULTIPHYSICS 4.4 to verify the cloaking effect. In our simulation model, the triangular object is with sound hard boundaries and the inclusion is the same as the background. It is then covered by the designed cloak and simulations are performed both in plane wave acoustic source and point acoustic source.

Figure 2(a) shows simulation results of the total acoustic pressure field of the triangular acoustic cloak with plane wave acoustic source at the frequency of 3000 Hz. For a perfect cloak ($r_0 = 0$), the parameters involves singularities. In order to avoid the singularities, r_0, r_1, and r_2 are chosen to be 0.02 m, 0.2 m, and 0.6 m, respectively. Equation (2) is applied to obtain the desired parameters of each segment. Layered structure is used in each segment to set the anisotropic density approximately. In Fig. 2(a), each segment of the cloak is divided into 20 layers, while each layer is composed of two different materials with the same thickness but different densities. With the effective medium theory[37] for layered structure

$$\begin{aligned} &(1+\eta)\rho_u = \rho_1 + \eta\rho_2, \\ &\frac{1+\eta}{\rho_v} = \frac{1}{\rho_1} + \frac{\eta}{\rho_2}, \\ &\frac{1+\eta}{B} = \frac{1}{B_1} + \frac{\eta}{B_2} \end{aligned} \tag{3}$$

where η is the thickness ratio of two materials and $\eta = 1$. To simplify the case, we set the bulk modulus of each region the same. Solving Eq. (3), we can obtain

$$\begin{aligned} &\rho_1 = \rho_u + \sqrt{\rho_u{}^2 - \rho_u\rho_v}, \\ &\rho_2 = \rho_u - \sqrt{\rho_u{}^2 - \rho_u\rho_v}, \\ &B_1 = B_2 = B \end{aligned} \tag{4}$$

for each segment to approximate the anisotropic parameters.

To make a comparison of the cloaking effect, Fig. 2(b) shows the total acoustic pressure field of the same plane wave acoustic source for a big triangular obstacle with circumradius of r_1. From Fig. 2(b), it can be clearly seen that the big triangular obstacle with circumradius of r_1 will

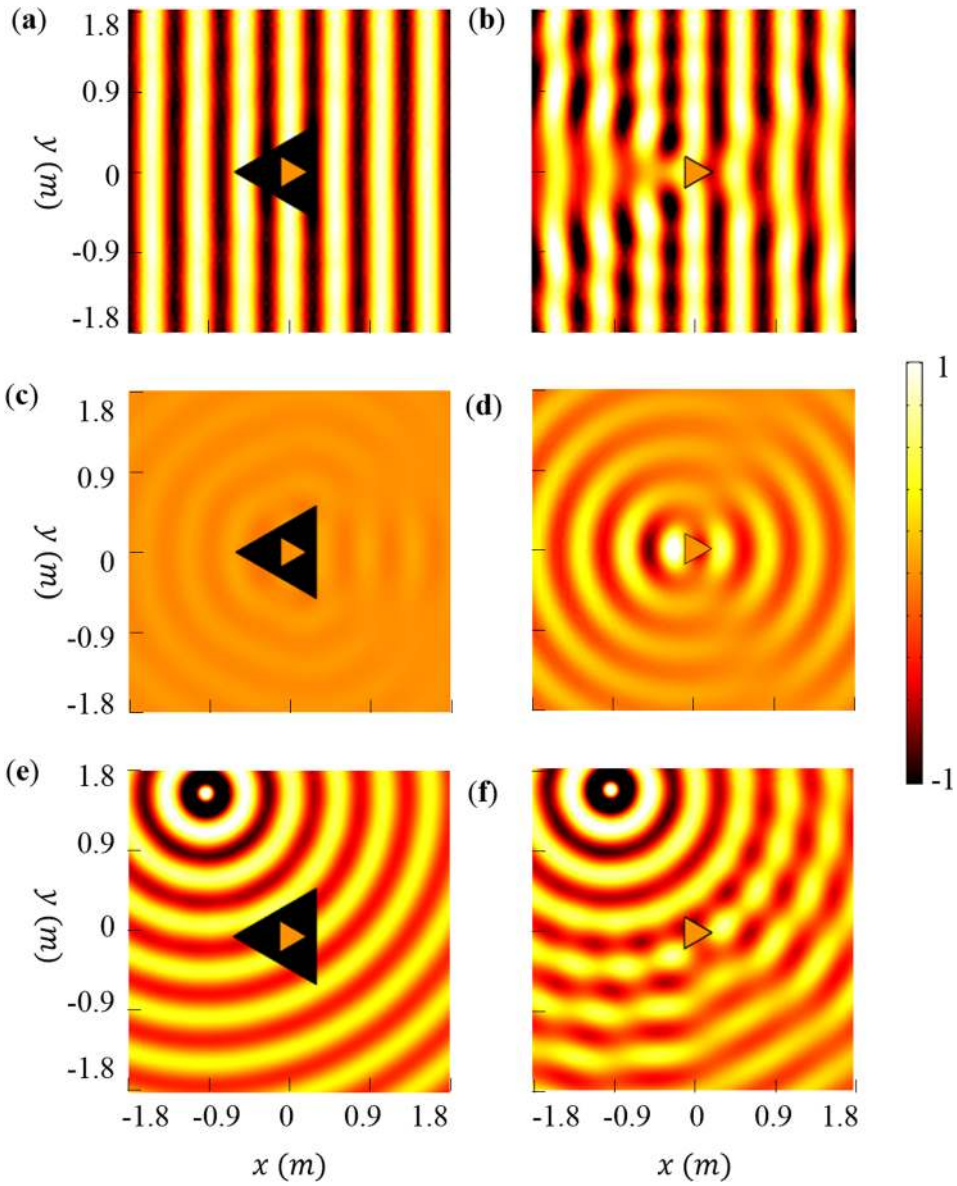

FIG. 2. (Color online) Total acoustic pressure field with plane wave source through (a) triangular acoustic cloak and (b) triangular obstacle with $r_1 = 0.2$ m. (c),(d) Scattered acoustic pressure field of (a) and (b), respectively. (e),(f) Same as (a) and (b) but with point source 1.8 m away from the middle and located at top left. The frequency is 3000 Hz.

disturb the wave front of the plane wave acoustic source and the wave is strongly scattered. Figures 2(c) and 2(d) show the scattered acoustic pressure field for Figs. 2(a) and 2(b), respectively. Compare Figs. 2(c) and 2(d), we can see that the scattering of the big obstacle is reduced with the triangular acoustic cloak. Since r_0 is much smaller than the wavelength here, the cloak has almost perfect performance to make the obstacle hard to be detected.

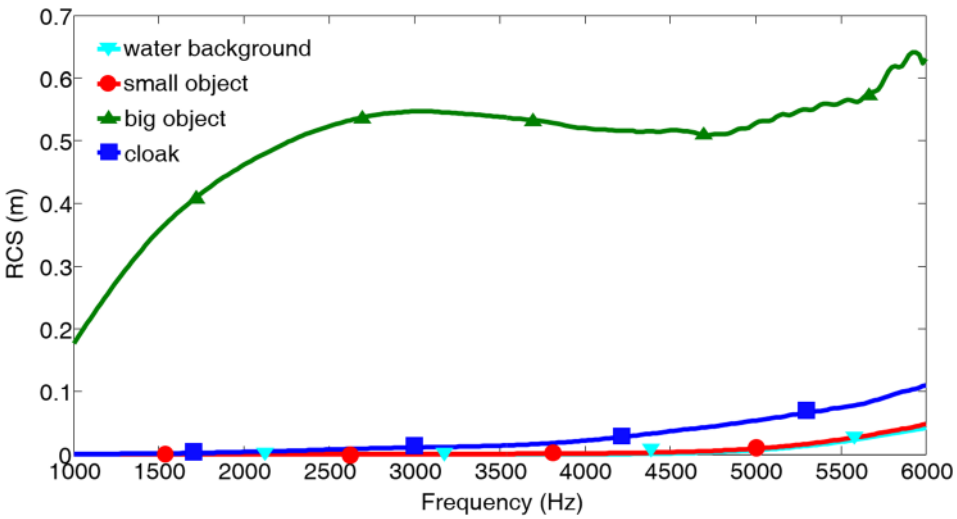

FIG. 3. (Color online) Line integral to calculate radar cross section (RCS) of cloak to illustrate the effect of acoustic cloak.

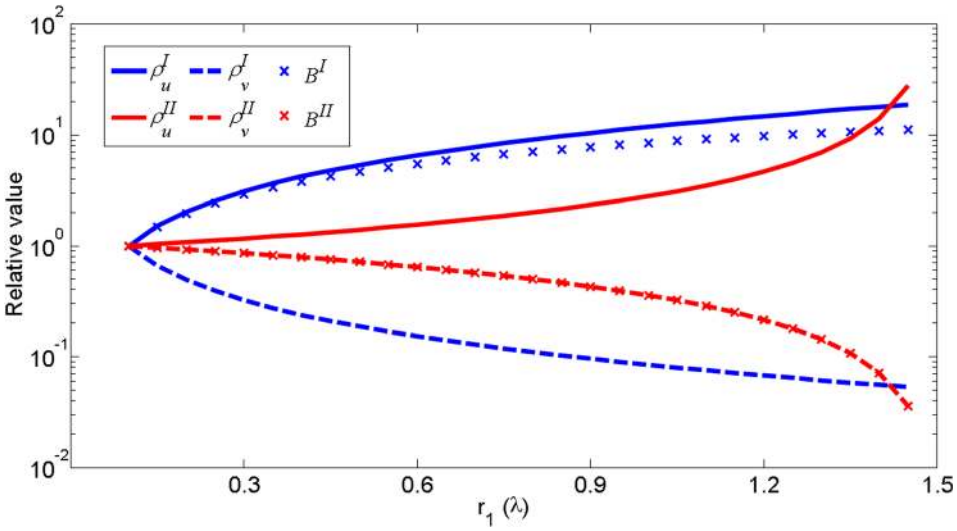

FIG. 4. (Color online) Relative values of the parameters as r_1 varies, where $r_0 = 0.1\lambda$ and $r_2 = 3\lambda$ are fixed.

Furthermore, in order to show the omnidirectional cloaking effect, simulation is also performed at the same frequency with a point source located at the top left. The results are shown in Figs. 2(e) and 2(f), from which we can see that the wave front of the point acoustic source is maintained with the cloak, verifying the cloaking effect for different angles.

We have calculated the radar cross section (RCS) of the cloak to quantitatively assess the effect of acoustic cloak. Here, the plane wave source is used at the frequency from 1000 to 6000 Hz while the big obstacle and small obstacle are with circumradius of $r_1 = 0.2$ m and $r_0 = 0.02$ m, respectively. RCS is defined as $\sigma_{\text{total}} = \int \lim_{r\to\infty} 2\pi r(|p_s|^2)/(|p_i|^2)d\theta$, since the power is distributed in the shape of a circle in two-dimensions, r represents the radius of the circle, p_s represents scattered pressure field, and p_i represents incident pressure field in the range r. The results in Fig. 3 show the RCS ratio is reduced more than 80% from 1000 to 6000 Hz. It should be noted that the RCS of the cloak gets a little higher in high frequencies since the effective medium theory works better in low frequency than that in high frequency where the wavelength will be comparable to the thickness of each layer.

IV. EXAMPLE OF IMPLEMENTATION

From Eq. (2), we can see the anisotropic factors of the densities $\rho_u^{I'}/\rho_v^{I'}$ and $\rho_u^{II'}/\rho_v^{II'}$ are related to the ratio of r_0/r_1. If r_1 is fixed, when r_0 gets smaller, the performance of the cloak will be better but the parameters of the cloak will have a larger anisotropic factor that makes the cloak difficult for practical realization. When r_0 and r_2 are fixed to be $r_0 = 0.1\lambda$ and $r_2 = 3\lambda$, Fig. 4 shows the relative values of the parameters as r_1 varies from r_0 to $r_2/2$. We can clearly see from Fig. 4 that the value of ρ_u^I, ρ_u^{II}, and B^I get bigger very fast as r_1 increased, while ρ_v^I, ρ_v^{II}, and B^{II} get smaller at the same time. In nature, we can hardly find the materials satisfying these highly anisotropic parameters.

Nevertheless, compared with inhomogeneous cloak, the parameters obtained from this method are much easier to realize. Here, we propose a design of the unit cells for acoustic cloak with realizable material parameters. By choosing $r_2 = 0.6$ m, $r_1 = 0.2$ m, and $r_0 = 0.1$ m, we can get the required parameters for each section from Eq. (2),

$$\begin{aligned}&\text{For segment I}: \rho_u^{I'} = 2.2\rho_0, \rho_v^{I'} = 0.45\rho_0, B^{I'} = 1.82B_0,\\ &\text{For segment II}: \rho_u^{II'} = 2\rho_0, \rho_v^{II'} = 0.5\rho_0, B^{II'} = 0.5B_0.\end{aligned} \tag{5}$$

Although in this case the cloak will not have an ideal cloaking effect because r_0 and r_1 are close, the cloak will still be effective to reduce the scattering of the big triangular obstacle. Furthermore, we can see that the required parameters in each section have the potential feasibility for practical realization.

We choose the background of the whole area to be water, with a density of $\rho_0 = 1000\,\text{kg/m}^3$ and bulk modulus of $B_0 = 2.25$ GPa. To realize the less than unity mass densities, aluminum foam characterized by $\rho = 240\,\text{kg/m}^3$, $B_0 = 2.5$ GPa, and nickel foam with $\rho = 300\,\text{kg/m}^3$, $B = 0.8$ GPa are used, which are all air filled foams and commercially available.[38] The material denser than water is steel with $\rho = 7910\,\text{kg/m}^3$, $B = 202$ GPa. The reason why we choose two different types of metal foams is to obtain the acoustic metamaterials characterized by Eq. (5) with different effective bulk modulus in each segment.

The unit cells for each segment are square with a period of $L = 25$ mm, which are highly subwavelength around the frequency of 2000 Hz. The structures of the unit cells are shown in Fig. 5(a), each of which is composed of steel and one kind of air-filled metal foam. Figure 5(b) shows the effective properties for each unit cell. We can see that the parameters do not change very much in frequency band from 1000 to 3000 Hz. The unit cell for segment I has effective parameters $\rho_u^I = 0.46\rho_0$, $\rho_v^I = 2.24\rho_0$, $B^I = 1.57B_0$, while the unit cell for segment II has effective parameters

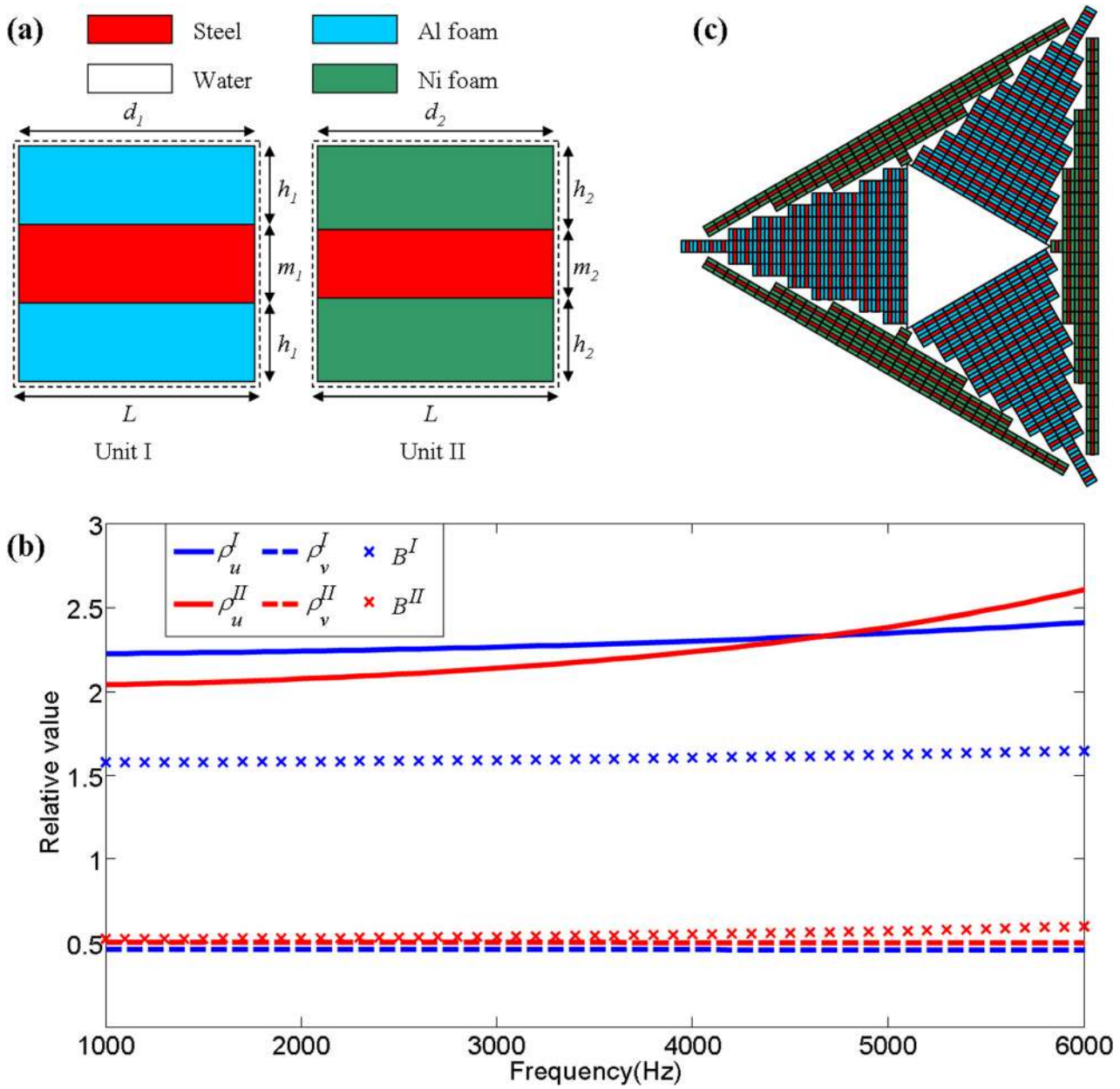

FIG. 5. (Color online) (a) The structures of unit cells for each segment. Each unit cell is composed of steel and one kind of metal foam while the background is water, with $L = 25$ mm, $d_1 = d_2 = 24$ mm, $m_1 = h_1 = 8$ mm, $m_2 = 7$ mm, and $h_2 = 8.5$ mm. (b) The effective properties of each unit cell. The parameters do not change very much in a broad frequency band. (c) The structure of the whole device filled with unit cells.

$\rho_u^{II} = 0.5\rho_0$, $\rho_v^{II} = 2.08\rho_0$, $B^{II} = 0.52B_0$ at 2000 Hz, which are within 5% of the density and 15% of the bulk modulus specified by Eq. (5). It should be noted that the flexibility of the solid frame is neglected and we just considered the unit cells as the linear elastic fluids in the simulation. The structure of the whole device with these unit cells is shown in Fig. 5(c).

Numerical simulation for the cloak with designed unit cells is also performed and the results are shown in Fig. 6 at the frequency of 2000 Hz. Figure 6(a) shows the total acoustic pressure field of the acoustic cloak with the structure in Fig. 5(c), while Fig. 6(b) is the case of a big triangular obstacles with circumradius of $r_1 = 0.2$ m. Figures 6(c) and 6(d) show the scattered acoustic field for Figs. 6(a) and 6(b), respectively. We can see that the cloak with realizable metamaterial is still effective to reduce the scattering of big obstacle. It should also be noted that although the unit cells cannot fully fill the volume of the cloak, the performance of the cloak is still acceptable when we chose this simple filling strategy.

Here, RCSs are also calculated as shown in Fig. 6(e). It shows the same tendency as in Fig. 3, and the RCS of the cloak is greatly reduced compared with the big obstacle especially in the low frequency band. The RCS ratio is reduced more than 50% in the frequency band from 1000 to 3400 Hz, while it is reduced more than 80% from 1000 to 2000 Hz.

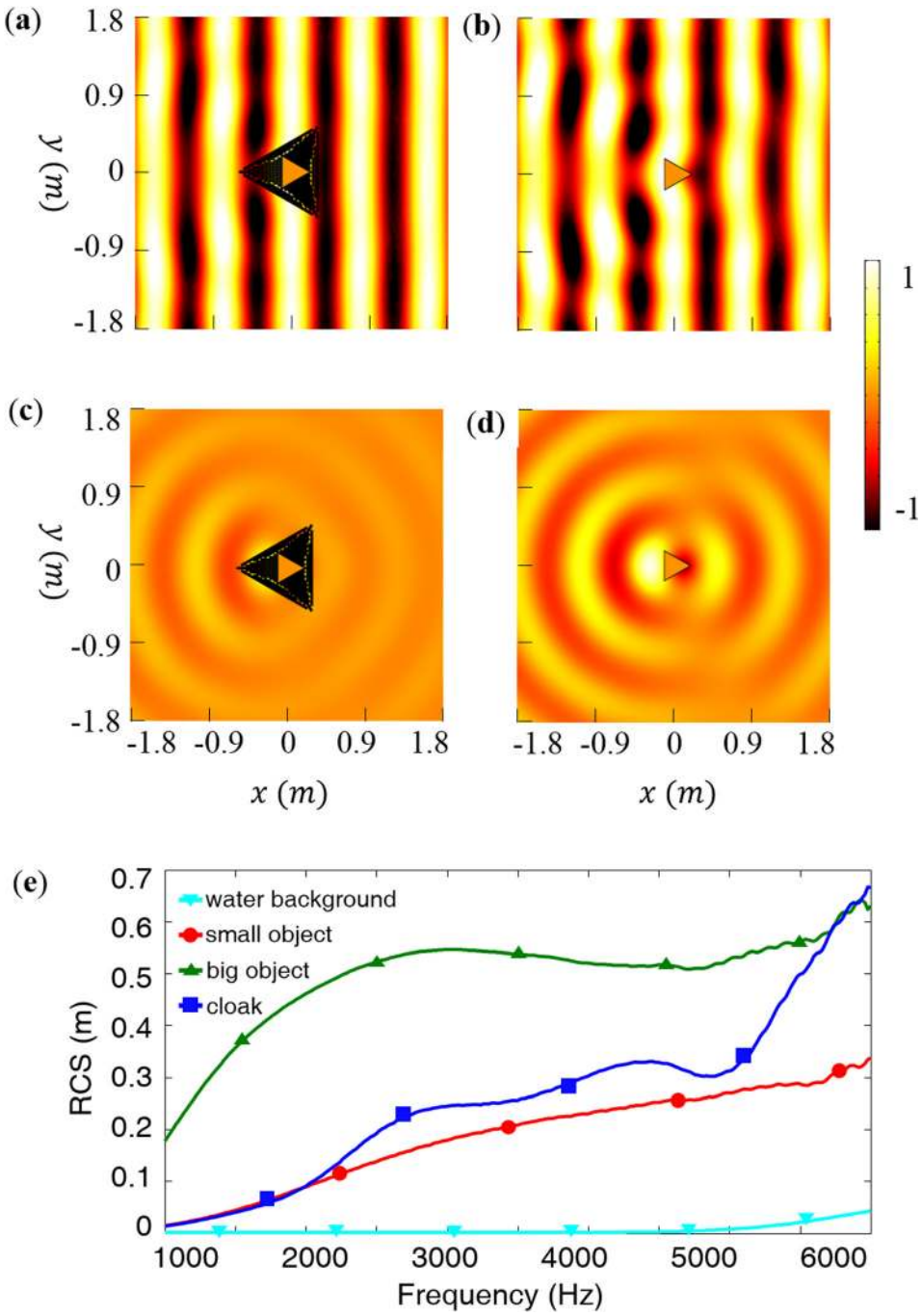

FIG. 6. (Color online) Total acoustic pressure field of (a) the cloak with realizable metamaterials and (b) the triangular obstacle. (c), (d) Scattered acoustic pressure field of (a) and (b), respectively. The plane wave source is at the frequency of 2000 Hz. (e) Calculated RCS for the acoustic cloak with realizable metamaterials.

V. CONCLUSION

In conclusion, we designed an acoustic polygonal cloak by using a linear transformation method. The cloak is divided into several different segments, all of which are with homogeneous and anisotropic parameters. Furthermore, we demonstrated a way to design the segments of the cloak with commercially available materials. Simulation results showed that the designed acoustic cloak is effective to reduce the scattering of big obstacle. The result shows that the RCS ratio is reduced more than 50% in the frequency band from 1000 to 3400 Hz, while it is reduced more than 80% from 1000 to 2000 Hz. This indicates the broad bandwidth of the cloak.

ACKNOWLEDGMENT

This work was sponsored by the National Natural Science Foundation of China under Grant Nos. 61322501, 61574127, and 61275183, the Top-Notch Young Talents Program of China, the Program for New Century Excellent Talents (NCET-12-0489) in University, the Fundamental Research Funds for the Central Universities, the Innovation Joint Research Center for Cyber-Physical-Society System, and the Postdoctoral Science Foundation of China under Grant No. 2015M581930. C.M., J.X., and N.F. acknowledge the Multidisciplinary University Research Initiative from the Office of Naval Research for financial support through Grant No. N00014-13-1-0631.

[1]J. B. Pendry, D. Schurig, and D. R. Smith, "Controlling electromagnetic fields," Science **312**, 1780–1782 (2006).
[2]U. Leonhardt, "Optical conformal mapping," Science **312**, 1777–1780 (2006).
[3]D. Schurig, J. J. Mock, B. J. Justice, S. A. Cummer, J. B. Pendry, A. F. Starr, and D. R. Smith, "Metamaterial electromagnetic cloak at microwave frequencies," Science **314**, 977–980 (2006).
[4]J. Li and J. B. Pendry, "Hiding under the carpet: A new strategy for cloaking," Phys. Rev. Lett. **101**, 203901 (2008).
[5]B. Kanté, D. Germain, and A. de Lustrac, "Experimental demonstration of a nonmagnetic metamaterial cloak at microwave frequencies," Phys. Rev. B **80**, 201104 (2009).
[6]H. F. Ma and T. J. Cui, "Three-dimensional broadband ground-plane cloak made of metamaterials," Nat. Commun. **1**, 21 (2010).
[7]X. Chen, Y. Luo, J. Zhang, K. Jiang, J. B. Pendry, and S. Zhang, "Macroscopic invisibility cloaking of visible light," Nat. Commun. **2**, 176 (2011).
[8]B. Zhang, Y. Luo, X. Liu, and G. Barbastathis, "Macroscopic invisibility cloak for visible light," Phys. Rev. Lett. **106**, 033901 (2011).
[9]H. Chen, B. Zheng, L. Shen, H. Wang, X. Zhang, N. I. Zheludev, and B. Zhang, "Ray-optics cloaking devices for large objects in incoherent natural light," Nat. Commun. **4**, 2652 (2013).
[10]N. Landy and D. R. Smith, "A full-parameter unidirectional metamaterial cloak for microwaves," Nat. Mater. **12**, 25–28 (2013).
[11]W. X. Jiang, W. X. Tang, and T. J. Cui, "Transformation optics and applications in microwave frequencies," Prog. Electromagn. Res. **149**, 251–273 (2014).
[12]R. Fleury and A. Alù, "Cloaking and invisibility: A review," Prog. Electromagn. Res. **147**, 171–202 (2014).
[13]H. Y. Chen and C. T. Chan, "Acoustic cloaking in three dimensions using acoustic metamaterials," Appl. Phys. Lett. **91**, 183518 (2007).
[14]S. A. Cummer and D. Schurig, "One path to acoustic cloaking," New J. Phys. **9**, 45 (2007).
[15]H. Y. Chen and C. T. Chan, "Acoustic cloaking and transformation acoustics," J. Phys. D: Appl. Phys. **43**, 113001 (2010).
[16]N. H. Gokhale, J. L. Cipolla, and A. N. Norris, "Special transformations for pentamode acoustic cloaking," J. Acoust. Soc. Am. **132**, 2932–2941 (2012).
[17]Y. Cheng, F. Yang, J. Y. Xu, and X. J. Liu, "A multilayer structured acoustic cloak with homogeneous isotropic materials," Appl. Phys. Lett. **92**, 151913 (2008).
[18]S. A. Cummer, B. I. Popa, D. Schurig, D. R. Smith, J. Pendry, M. Rahm, and A. Starr, "Scattering theory derivation of a 3D acoustic cloaking shell," Phys. Rev. Lett. **100**, 024301 (2008).
[19]A. N. Norris, "Acoustic cloaking theory," Proc. R. Soc. A **464**, 2411–2434 (2008).
[20]J. B. Pendry and J. Li, "An acoustic metafluid: Realizing a broadband acoustic cloak," New J. Phys. **10**, 115032 (2008).
[21]D. Torrent and J. Sanchez-Dehesa, "Acoustic cloaking in two dimensions: A feasible approach," New J. Phys. **10**, 063015 (2008).
[22]S. Zhang, C. Xia, and N. Fang, "Broadband acoustic cloak for ultrasound waves," Phys. Rev. Lett. **106**, 024301 (2011).
[23]B. I. Popa and S. A. Cummer, "Homogeneous and compact acoustic ground cloaks," Phys. Rev. B **83**, 224304 (2011).
[24]B. I. Popa, L. Zigoneanu, and S. A. Cummer, "Experimental acoustic ground cloak in air," Phys. Rev. Lett. **106**, 253901 (2011).
[25]X. L. Zhang, X. Ni, M. H. Lu, and Y. F. Chen, "A feasible approach to achieve acoustic carpet cloak in air," Phys. Lett. A **376**, 493–496 (2012).
[26]L. Zigoneanu, B. I. Popa, and S. A. Cummer, "Three-dimensional broadband omnidirectional acoustic ground cloak," Nat. Mater. **13**, 352–355 (2014).
[27]J. Xu, X. Jiang, N. Fang, E. Georget, R. Abdeddaim, J. M. Geffrin, M. Farhat, P. Sabouroux, S. Enoch, and S. Guenneau, "Molding acoustic, electromagnetic and water waves with a single cloak," Sci. Rep. **5**, 10678 (2015).
[28]C. A. Rohde, T. P. Martin, M. D. Guild, C. N. Layman, C. J. Naify, M. Nicholas, A. L. Thangawng, D. C. Calvo, and G. J. Orris, "Experimental demonstration of underwater acoustic scattering cancellation," Sci. Rep. **5**, 13175 (2015).
[29]S. Xi, H. S. Chen, B. I. Wu, and J. A. Kong, "One-directional perfect cloak created with homogeneous material," IEEE Microwave Wireless Compon. **19**, 131–133 (2009).
[30]Y. Luo, J. J. Zhang, H. S. Chen, L. X. Ran, B. I. Wu, and J. A. Kong, "A rigorous analysis of plane-transformed invisibility cloaks," IEEE Trans. Antennas Propag. **57**, 3926–3933 (2009).
[31]X. F. Xu, Y. J. Feng, Y. Hao, J. M. Zhao, and T. Jiang, "Infrared carpet cloak designed with uniform silicon grating structure," Appl. Phys. Lett. **95**, 184102 (2009).
[32]W. Li, J. G. Guan, Z. G. Sun, W. Wang, and Q. J. Zhang, "A near-perfect invisibility cloak constructed with homogeneous materials," Opt. Exp. **17**, 26 (2009).
[33]X. H. Wang, S. Qu, X. Wu, J. F. Wang, Z. Xu, and H. Ma, "Broadband three-dimensional diamond-shaped invisible cloaks composed of tetrahedral homogeneous blocks," J. Phys. D: Appl. Phys. **43**, 305501 (2010).
[34]W. R. Zhu, C. L. Ding, and X. P. Zhao, "A numerical method for designing acoustic cloak with homogeneous metamaterials," Appl. Phys. Lett. **97**, 131902 (2010).
[35]T. H. Li, M. Huang, J. J. Yang, Y. Z. Lan, and J. Sun, "Homogeneous material constructed acoustic cloak based on coordinate transformation," J. Vib. Acoust. **134**, 051016 (2012).
[36]H. Chen and B. Zheng, "Broadband polygonal invisibility cloak for visible light," Sci. Rep. **2**, 255 (2012).
[37]M. Schoenberg and P. N. Sen, "Properties of a periodically stratified acoustic half-space and its relation to a Biot fluid," J. Acoust. Soc. Am. **73**, 61–67 (1983).
[38]M. F. Ashby, T. Evans, N. A. Fleck, J. Hutchinson, H. Wadley, and L. Gibson, *Metal Foams: A Design Guide* (Elsevier, New York, 2000), pp. 40–44.